Positivity-preserving high order schemes for convection dominated equations

Chi-Wang Shu

Division of Applied Mathematics

Brown University

Joint work with Xiangxiong Zhang; Yinhua Xia; Yulong Xing; Cheng Wang and Jianguo Ning; Yuanyuan Liu; Yifan Zhang; Rui Zhang and Mengping Zhang; Jingmei Qiu

Outline

- Introduction
- Maximum-principle-preserving for scalar conservation laws
- Convection-diffusion equations
- Positivity-preserving for systems
- Other generalizations
- Numerical results
- Conclusions and future work

Introduction

For the scalar conservation laws

$$u_t + \nabla \cdot \mathbf{F}(u) = 0, \qquad u(\mathbf{x}, 0) = u_0(\mathbf{x}). \tag{1}$$

An important property of the entropy solution (which may be discontinuous) is that it satisfies a strict maximum principle: If

$$M = \max_{\mathbf{x}} u_0(\mathbf{x}), \quad m = \min_{\mathbf{x}} u_0(\mathbf{x}), \tag{2}$$

then $u(\mathbf{x}, t) \in [m, M]$ for any $\mathbf{x}$ and t.

First order monotone schemes can maintain the maximum principle. For the one-dimensional conservation law

$$u_t + f(u)_x = 0,$$

the first order monotone scheme

$$\begin{aligned} u_j^{n+1} &= H_\lambda(u_{j-1}^n, u_j^n, u_{j+1}^n) \\ &= u_j^n - \lambda[h(u_j^n, u_{j+1}^n) - h(u_{j-1}^n, u_j^n)] \end{aligned}$$

where $\lambda = \frac{\Delta t}{\Delta x}$ and $h(u^-, u^+)$ is a monotone flux ($h(\uparrow, \downarrow)$), satisfies

$$H_\lambda(\uparrow, \uparrow, \uparrow)$$

under a suitable CFL condition

$$\lambda \leq \lambda_0.$$

Therefore, if

$$m \leq u_{j-1}^n, u_j^n, u_{j+1}^n \leq M$$

then

$$u_j^{n+1} = H_\lambda(u_{j-1}^n, u_j^n, u_{j+1}^n) \geq H_\lambda(m, m, m) = m,$$

and

$$u_j^{n+1} = H_\lambda(u_{j-1}^n, u_j^n, u_{j+1}^n) \leq H_\lambda(M, M, M) = M.$$

However, for higher order linear schemes, i.e. schemes which are linear for a linear PDE

$$u_t + a u_x = 0 \tag{3}$$

for example the second order accurate Lax-Wendroff scheme

$$u_j^{n+1} = \frac{a\lambda}{2}(1 + a\lambda)u_{j-1}^n + (1 - a^2\lambda^2)u_j^n - \frac{a\lambda}{2}(1 - a\lambda)u_{j+1}^n$$

where $\lambda = \frac{\Delta t}{\Delta x}$ and $|a|\lambda \leq 1$, the maximum principle is not satisfied. In fact, no linear schemes with order of accuracy higher than one can satisfy the maximum principle (Godunov Theorem).

Therefore, nonlinear schemes, namely schemes which are nonlinear even for linear PDEs, have been designed to overcome this difficulty. These include roughly two classes of schemes:

- TVD schemes. Most TVD (total variation diminishing) schemes also satisfy strict maximum principle, even in multi-dimensions. TVD schemes can be designed for any formal order of accuracy for solutions in smooth, monotone regions. However, all TVD schemes will degenerate to first order accuracy at smooth extrema.
- TVB schemes, ENO schemes, WENO schemes. These schemes do not insist on strict TVD properties, therefore they do not satisfy strict maximum principles, although they can be designed to be arbitrarily high order accurate for smooth solutions.

Remark: If we insist on the maximum principle interpreted as

$$m \leq u_j^{n+1} \leq M, \qquad \forall j$$

if

$$m \leq u_j^{n} \leq M, \qquad \forall j,$$

where u_j^n is either the approximation to the point value $u(x_j, t^n)$ for a finite difference scheme, or to the cell average $\frac{1}{\Delta x}\int_{x_{j-1/2}}^{x_{j+1/2}} u(x, t^n)dx$ for a finite volume or DG scheme, then the scheme can be at most second order accurate (proof due to Harten, see Zhang and Shu, Proceedings of the Royal Society A, 2011).

Therefore, the correct procedure to follow in designing high order schemes that satisfy a strict maximum principle is to change the definition of maximum principle. Note that a high order finite volume scheme has the following algorithm flowchart:

(1) Given $\{\bar{u}_j^n\}$

(2) reconstruct $u^n(x)$ (piecewise polynomial with cell average $\bar{u}_j^n$)

(3) evolve by, e.g. Runge-Kutta time discretization to get $\{\bar{u}_j^{n+1}\}$

(4) return to (1)

Therefore, instead of requiring

$$m \leq \bar{u}_j^{n+1} \leq M, \qquad \forall j$$

if

$$m \leq \bar{u}_j^{n} \leq M, \qquad \forall j,$$

we will require

$$m \leq u^{n+1}(x) \leq M, \qquad \forall x$$

if

$$m \leq u^{n}(x) \leq M, \qquad \forall x.$$

Similar definition and procedure can be used for discontinuous Galerkin schemes.

Maximum-principle-preserving for scalar conservation laws

The flowchart for designing a high order scheme which obeys a strict maximum principle is as follows:

1. Start with $u^n(x)$ which is high order accurate

$$|u(x,t^n) - u^n(x)| \leq C\Delta x^p$$

and satisfy

$$m \leq u^n(x) \leq M, \qquad \forall x$$

therefore of course we also have

$$m \leq \bar{u}_j^n \leq M, \qquad \forall j.$$

2. Evolve for one time step to get

$$m \leq \bar{u}_j^{n+1} \leq M, \qquad \forall j. \tag{4}$$

3. Given (4) above, obtain the reconstruction $u^{n+1}(x)$ which

   - satisfies the maximum principle

$$m \leq u^{n+1}(x) \leq M, \qquad \forall x;$$

   - is high order accurate

$$|u(x, t^{n+1}) - u^{n+1}(x)| \leq C\Delta x^p.$$

Three major difficulties

1. The first difficulty is how to evolve in time for one time step to guarantee

$$m \leq \bar{u}_j^{n+1} \leq M, \qquad \forall j. \tag{5}$$

This is very difficult to achieve. Previous works use one of the following two approaches:

- Use exact time evolution. This can guarantee

$$m \leq \bar{u}_j^{n+1} \leq M, \qquad \forall j.$$

However, it can only be implemented with reasonable cost for linear PDEs, or for nonlinear PDEs in one dimension. This approach was used in, e.g., Jiang and Tadmor, SISC 1998; Liu and Osher, SINUM 1996; Sanders, Math Comp 1988; Qiu and Shu, SINUM 2008; Zhang and Shu, SINUM 2010; to obtain TVD schemes or maximum-principle-preserving schemes for linear and nonlinear PDEs in one dimension or for linear PDEs in multi-dimensions, for second or third order accurate schemes.

- Use simple time evolution such as SSP Runge-Kutta or multi-step methods. However, additional limiting will be needed on $u^n(x)$ which will destroy accuracy near smooth extrema.

We have figured out a way to obtain

$$m \leq \bar{u}_j^{n+1} \leq M, \qquad \forall j$$

with simple Euler forward or SSP Runge-Kutta or multi-step methods without losing accuracy on the limited $u^n(x)$:

The evolution of the cell average for a higher order finite volume or DG scheme satisfies

$$\begin{aligned} \bar{u}_j^{n+1} &= G(\bar{u}_j^n, u^-_{j-\frac{1}{2}}, u^+_{j-\frac{1}{2}}, u^-_{j+\frac{1}{2}}, u^+_{j+\frac{1}{2}}) \\ &= \bar{u}_j^n - \lambda[h(u^-_{j+\frac{1}{2}}, u^+_{j+\frac{1}{2}}) - h(u^-_{j-\frac{1}{2}}, u^+_{j-\frac{1}{2}})], \end{aligned}$$

where

$$G(\uparrow, \uparrow, \downarrow, \downarrow, \uparrow)$$

therefore there is no maximum principle. The problem is with the two arguments $u^+_{j-\frac{1}{2}}$ and $u^-_{j+\frac{1}{2}}$ which are values at points inside the cell I_j.

The polynomial $p_j(x)$ (either reconstructed in a finite volume method or evolved in a DG method) is of degree k, defined on I_j such that $\bar{u}_j^n$ is its cell average on I_j, $u^+_{j-\frac{1}{2}} = p_j(x_{j-\frac{1}{2}})$ and $u^-_{j+\frac{1}{2}} = p_j(x_{j+\frac{1}{2}})$.

We take a Legendre Gauss-Lobatto quadrature rule which is exact for polynomials of degree k, then

$$\bar{u}_j^n = \sum_{\ell=0}^{m} \omega_\ell p_j(y_\ell)$$

with $y_0 = x_{j-\frac{1}{2}}$, $y_m = x_{j+\frac{1}{2}}$. The scheme for the cell average is then rewritten as

$$
\begin{aligned}
\bar{u}_j^{n+1} &= \omega_m \left[u^-_{j+\frac{1}{2}} - \frac{\lambda}{\omega_m} \left(h(u^-_{j+\frac{1}{2}}, u^+_{j+\frac{1}{2}}) - h(u^+_{j-\frac{1}{2}}, u^-_{j+\frac{1}{2}}) \right) \right] \\
&\quad + \omega_0 \left[u^+_{j-\frac{1}{2}} - \frac{\lambda}{\omega_0} \left(h(u^+_{j-\frac{1}{2}}, u^-_{j+\frac{1}{2}}) - h(u^-_{j-\frac{1}{2}}, u^+_{j-\frac{1}{2}}) \right) \right] \\
&\quad + \sum_{\ell=1}^{m-1} \omega_\ell p_j(y_\ell) \\
&= \omega_m H_{\lambda/\omega_m}(u^+_{j-\frac{1}{2}}, u^-_{j+\frac{1}{2}}, u^+_{j+\frac{1}{2}}) + \omega_0 H_{\lambda/\omega_0}(u^-_{j-\frac{1}{2}}, u^+_{j-\frac{1}{2}}, u^-_{j+\frac{1}{2}}) \\
&\quad + \sum_{\ell=1}^{m-1} \omega_\ell p_j(y_\ell).
\end{aligned}
$$

Therefore, if

$$m \leq p_j(y_\ell) \leq M$$

at all Legendre Gauss-Lobatto quadrature points and a reduced CFL condition

$$\lambda/\omega_m = \lambda/\omega_0 \leq \lambda_0$$

is satisfied, then

$$m \leq \bar{u}_j^{n+1} \leq M.$$

2. The second difficulty is: given

$$m \leq \bar{u}_j^{n+1} \leq M, \qquad \forall j$$

how to obtain an accurate reconstruction $u^{n+1}(x)$ which satisfy

$$m \leq u^{n+1}(x) \leq M, \qquad \forall x.$$

Previous work was mainly for relatively lower order schemes (second or third order accurate), and would typically require an evaluation of the extrema of $u^{n+1}(x)$, which, for a piecewise polynomial of higher degree, is quite costly.

We have figured out a way to obtain such reconstruction with a very simple scaling limiter, which only requires the evaluation of $u^{n+1}(x)$ at certain pre-determined quadrature points and does not destroy accuracy:

We replace $p_j(x)$ by the limited polynomial $\tilde{p}_j(x)$ defined by

$$\tilde{p}_j(x) = \theta_j(p_j(x) - \bar{u}_j^n) + \bar{u}_j^n$$

where

$$\theta_j = \min\left\{\left|\frac{M - \bar{u}_j^n}{M_j - \bar{u}_j^n}\right|, \left|\frac{m - \bar{u}_j^n}{m_j - \bar{u}_j^n}\right|, 1\right\},$$

with

$$M_j = \max_{x \in S_j} p_j(x), \qquad m_j = \min_{x \in S_j} p_j(x)$$

where S_j is the set of Legendre Gauss-Lobatto quadrature points of cell I_j.

Clearly, this limiter is just a simple scaling of the original polynomial around its average.

The following lemma, guaranteeing the maintenance of accuracy of this simple limiter, is proved in Zhang and Shu, JCP 2010a:

Lemma: Assume $\bar{u}_j^n \in [m, M]$ and $p_j(x)$ is an $O(\Delta x^p)$ approximation, then $\tilde{p}_j(x)$ is also an $O(\Delta x^p)$ approximation.

3. The third difficulty is how to generalize the algorithm and result to 2D (or higher dimensions). Algorithms which would require an evaluation of the extrema of the reconstructed polynomials $u^{n+1}(x, y)$ would not be easy to generalize at all.

   Our algorithm uses only explicit Euler forward or SSP (also called TVD) Runge-Kutta or multi-step time discretizations, and a simple scaling limiter involving just evaluation of the polynomial at certain quadrature points, hence easily generalizes to 2D or higher dimensions on structured or unstructured meshes, with strict maximum-principle-satisfying property and provable high order accuracy.

The technique has been generalized to the following situations maintaining uniformly high order accuracy:

- 2D scalar conservation laws on rectangular or triangular meshes with strict maximum principle (Zhang and Shu, JCP 2010a; Zhang, Xia and Shu, JSC 2012).
- 2D incompressible equations in the vorticity-streamfunction formulation (with strict maximum principle for the vorticity), and 2D passive convections in a divergence-free velocity field, i.e.

$$\omega_t + (u\omega)_x + (v\omega)_x = 0,$$

with a given divergence-free velocity field (u, v), again with strict maximum principle (Zhang and Shu, JCP 2010a; Zhang, Xia and Shu, JSC 2012).

Convection-diffusion equations

Generalization to convection-diffusion equations

$$u_t + f(u)_x = (a(u)u_x)_x, \qquad a(u) \geq 0$$

is possible but not straightforward.

Currently there are mainly two results.

- Maximum-principle-satisfying high order finite volume WENO schemes for convection-diffusion equations using a non-standard finite volume framework (Zhang, Liu and Shu, SISC 2012).

  This approach is based on evolving the double cell averages

$$\bar{\bar{u}}_i = \frac{1}{\Delta x^2} \int_{x_{i-\frac{1}{2}}}^{x_{i+\frac{1}{2}}} \left(\int_{x-\frac{\Delta x}{2}}^{x+\frac{\Delta x}{2}} u(\xi) d\xi \right) dx.$$

  The approach introduced before for conservation laws can then be directly generalized. This approach works in multi-dimensions as well, but only on structured meshes.

- Piecewise linear DG methods on arbitrary triangular meshes (Zhang, Zhang and Shu, JCP 2013). This method is uniformly second order accurate, works on any triangular meshes without minimum or maximum angle restrictions, and satisfies strict maximum principle.

  This appears to be the first successful result in obtaining uniform second order accurate finite element method on unrestricted triangulations for parabolic equations.

  There are attempts to generalize this result to higher order DG methods (Jue Yan).

Positivity-preserving for systems

The framework of establishing maximum-principle-satisfying schemes for scalar equations can be generalized to hyperbolic systems to preserve the positivity of certain physical quantities, such as density and pressure of compressible gas dynamics.

Compressible Euler equations:

$$u_t + f(u)_x = 0$$

with

$$u = \begin{pmatrix} \rho \\ \rho v \\ E \end{pmatrix}, \qquad f(u) = \begin{pmatrix} \rho v \\ \rho v^2 + p \\ v(E+p) \end{pmatrix},$$

where $E = e + \frac{1}{2}\rho v^2$. The internal energy e is related to density and pressure through the equation of states (EOS). For the ideal gas, we have $e = \frac{p}{\gamma - 1}$ with $\gamma = 1.4$ for air.

The main ingredients for designing positivity-preserving schemes for systems are:

- A first order explicit scheme which can keep the positivity of the desired quantities (e.g. density and pressure) under a suitable CFL condition.

  Examples include the Godunov scheme, Lax-Friedrichs scheme, kinetic scheme, HLLC scheme, etc.

- The quantity for which positivity is desired is one of the components of the conserved variable u (for example the density ρ), or is a concave function of the conserved variable u (for example the pressure p or the internal energy e). Under this assumption, the region of positivity of the desired quantities is a convex region in the u space.

With these ingredients, the technique to enforce maximum-principle for scalar equations can be directly generalized to enforce positivity of the desired quantities without affecting the high order accuracy of the finite volume or DG schemes.

Positivity-preserving finite volume or DG schemes have been designed for:

- One and multi-dimensional compressible Euler equations maintaining positivity of density and pressure (Zhang and Shu, JCP 2010b; Zhang, Xia and Shu, JSC 2012).
- One and two-dimensional shallow water equations maintaining non-negativity of water height and well-balancedness for problems with dry areas (Xing, Zhang and Shu, Advances in Water Resources 2010; Xing and Shu, Advances in Water Resources 2011).

- One and multi-dimensional compressible Euler equations with source terms (geometric, gravity, chemical reaction, radiative cooling) maintaining positivity of density and pressure (Zhang and Shu, JCP 2011).
- One and multi-dimensional compressible Euler equations with gaseous detonations maintaining positivity of density, pressure and reactant mass fraction, with a new and simplified implementation of the pressure limiter. DG computations are stable without using the TVB limiter (Wang, Zhang, Shu and Ning, JCP 2012).
- A minimum entropy principle satisfying high order scheme for gas dynamics equations (Zhang and Shu, Num Math 2012).

Other generalizations

- Positivity-preserving high order finite difference WENO schemes for compressible Euler equations (Zhang and Shu, JCP 2012).
- Simplified version for WENO finite volume schemes without the need to evaluate solutions at quadrature points inside the cell (Zhang and Shu, Proceedings of the Royal Society A, 2011).

- Positivity-preserving for PDEs involving global integral terms including a hierarchical size-structured population model (Zhang, Zhang and Shu, JCAM 2011) and Vlasov-Boltzmann transport equations (Cheng, Gamba and Proft, Math Comp, 2012).
- Positivity-preserving semi-Lagrangian schemes (Qiu and Shu, JCP 2011; Rossmanith and Seal, JCP 2011).
- Positivity-preserving first order and higher order Lagrangian schemes for multi-material flows (Cheng and Shu, JCP submitted).

Numerical results

Example 1. Accuracy check. For the incompressible Euler equation in the vorticity-streamfunction formulation, with periodic boundary condition and initial data $\omega(x, y, 0) = -2\sin(x)\sin(y)$ on the domain $[0, 2\pi] \times [0, 2\pi]$, the exact solution is $\omega(x, y, t) = -2\sin(x)\sin(y)$. We clearly observe the designed order of accuracy for this solution.

Table 1: Incompressible Euler equations. P^2 for vorticity, $t = 0.5$.

N×N	L^1 error	order	L^∞ error	order
16×16	5.12E-4	–	1.40E-3	–
32×32	3.75E-5	3.77	1.99E-4	2.81
64×64	3.16E-6	3.57	2.74E-5	2.86
128×128	2.76E-7	3.51	3.56E-6	2.94

Example 2. The vortex patch problem. We solve the incompressible Euler equations in $[0, 2\pi] \times [0, 2\pi]$ with the initial condition

$$\omega(x, y, 0) = \begin{cases} -1, & \frac{\pi}{2} \le x \le \frac{3\pi}{2}, \frac{\pi}{4} \le y \le \frac{3\pi}{4}; \\ 1, & \frac{\pi}{2} \le x \le \frac{3\pi}{2}, \frac{5\pi}{4} \le y \le \frac{7\pi}{4}; \\ 0, & \text{otherwise} \end{cases}$$

and periodic boundary conditions. The contour plots of the vorticity ω are given for $t = 10$. Again, we cannot observe any significant difference between the two results in the contour plots. The cut along the diagonal gives us a clearer view of the advantage in using the limiter.

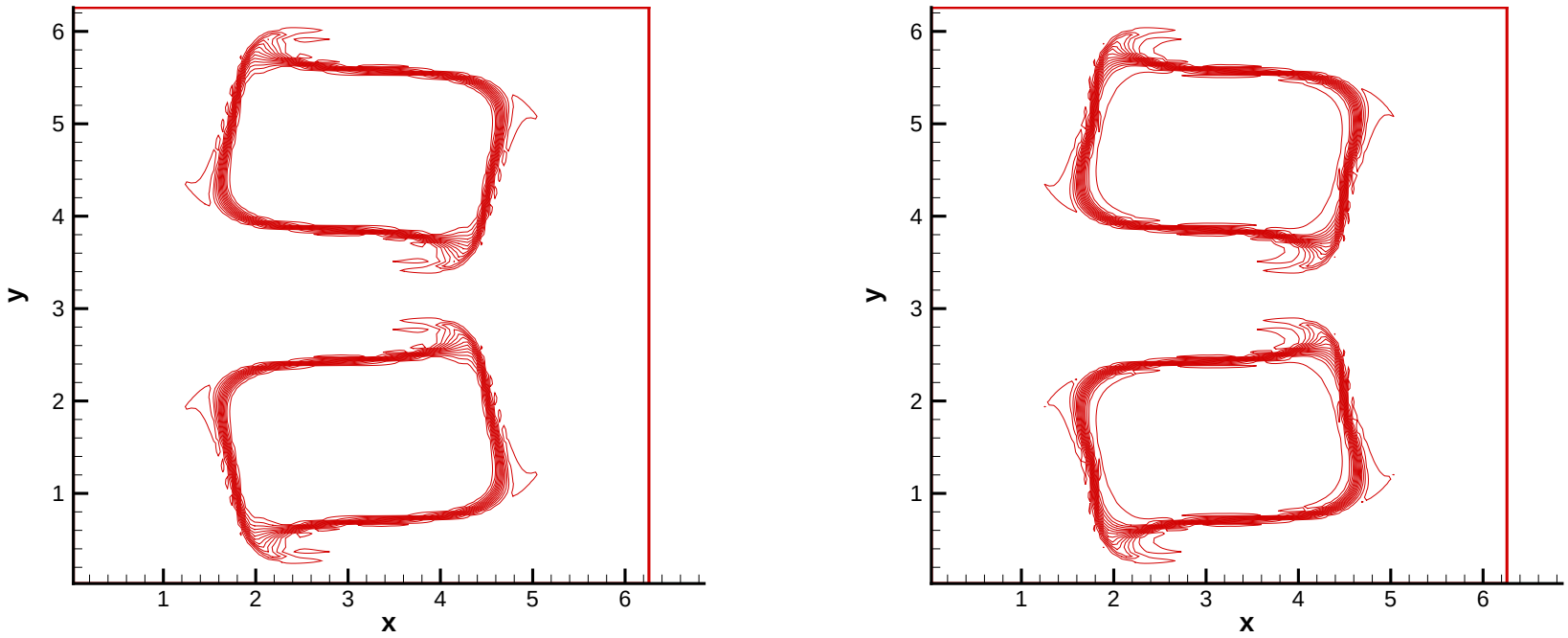

Figure 1: Vorticity at $t = 10$, P^2. 30 equally spaced contours from -1.1 to 1.1. 128^2 mesh. Left: with limiter; Right: without limiter.

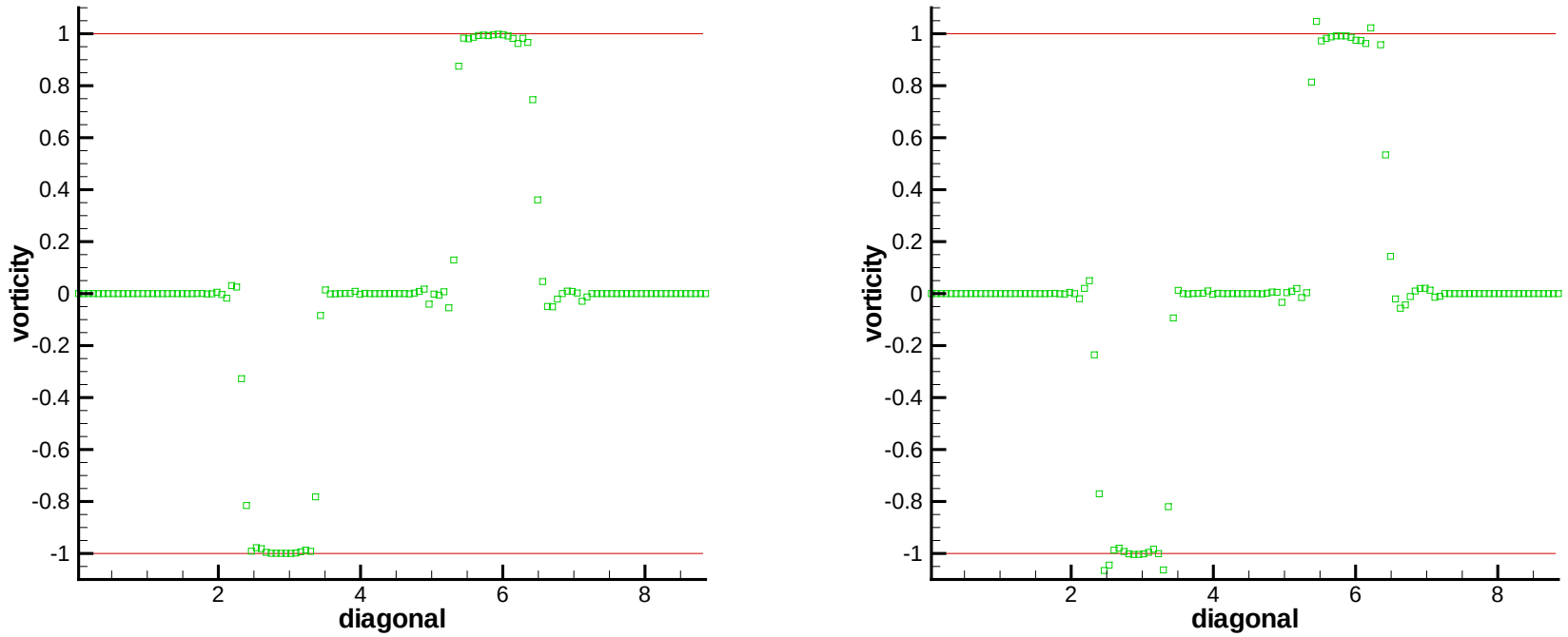

Figure 2: Vorticity at $t = 10$, P^2. Cut along the diagonal. 128^2 mesh. Left: with limiter; Right: without limiter.

Example 3. The Sedov point-blast wave in one dimension. For the initial condition, the density is 1, velocity is zero, total energy is 10^{-12} everywhere except that the energy in the center cell is the constant $\frac{E_0}{\Delta x}$ with $E_0 = 3200000$ (emulating a δ-function at the center). $\gamma = 1.4$. The computational results are shown in Figure 3. We can see the shock is captured very well.

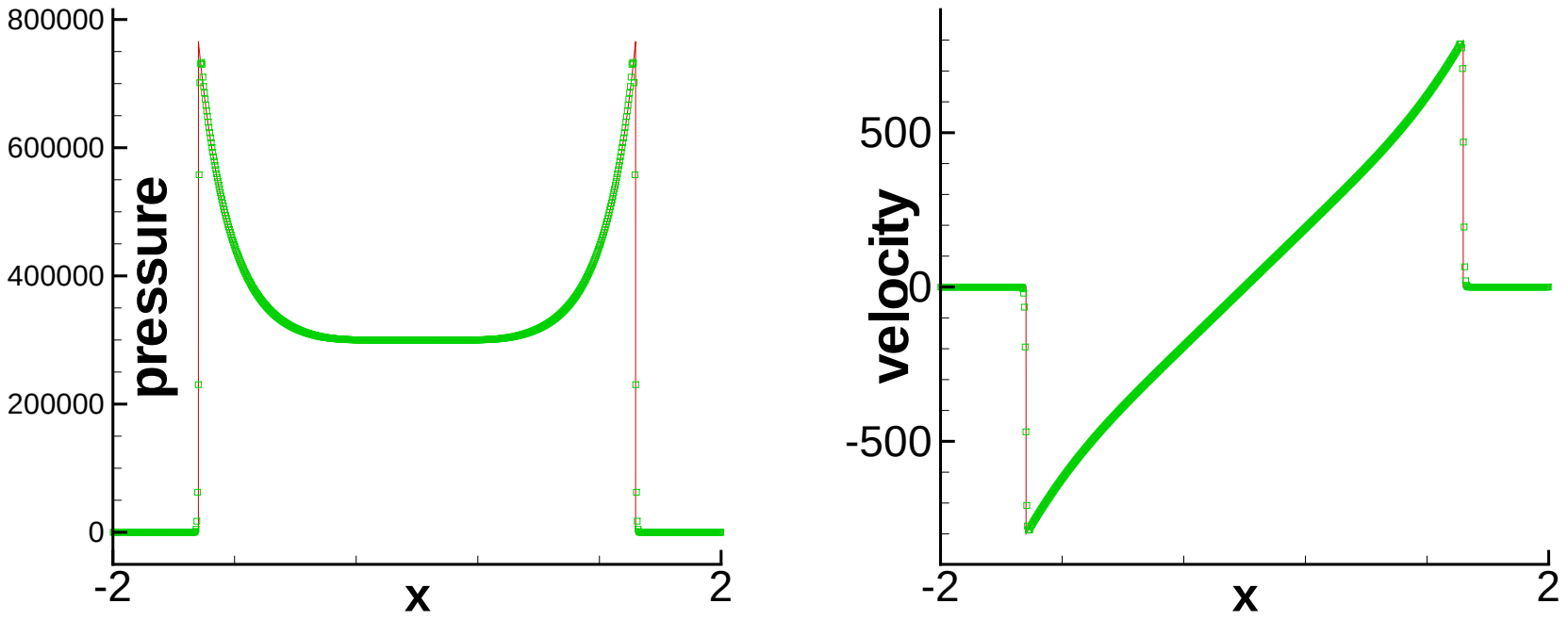

Figure 3: 1D Sedov blast. The solid line is the exact solution. Symbols are numerical solutions. $T = 0.001$. $N = 800$. $\Delta x = \frac{4}{N}$. TVB limiter parameters $(M_1, M_2, M_3) = (15000, 20000, 15000)$. Pressure (left) and velocity (right).

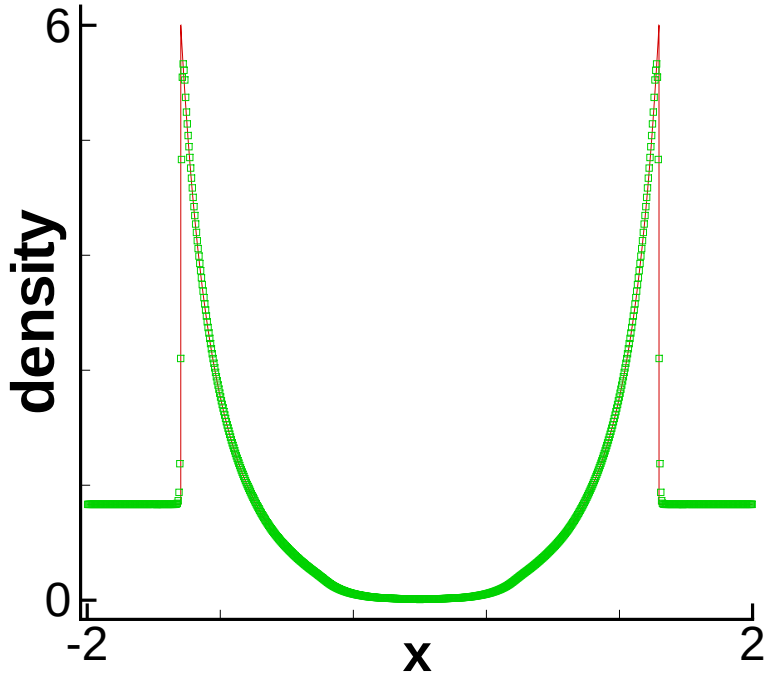

Figure 4: 1D Sedov blast. The solid line is the exact solution. Symbols are numerical solutions. $T = 0.001$. $N = 800$. $\Delta x = \frac{4}{N}$. TVB limiter parameters $(M_1, M_2, M_3) = (15000, 20000, 15000)$. Density.

Example 4. The Sedov point-blast wave in two dimensions. The computational domain is a square. For the initial condition, the density is 1, velocity is zero, total energy is 10^{-12} everywhere except that the energy in the lower left corner cell is the constant $\frac{0.244816}{\Delta x \Delta y}$. $\gamma = 1.4$. See Figure 5. The computational result is comparable to those in the literature, e.g. those computed by Lagrangian methods.

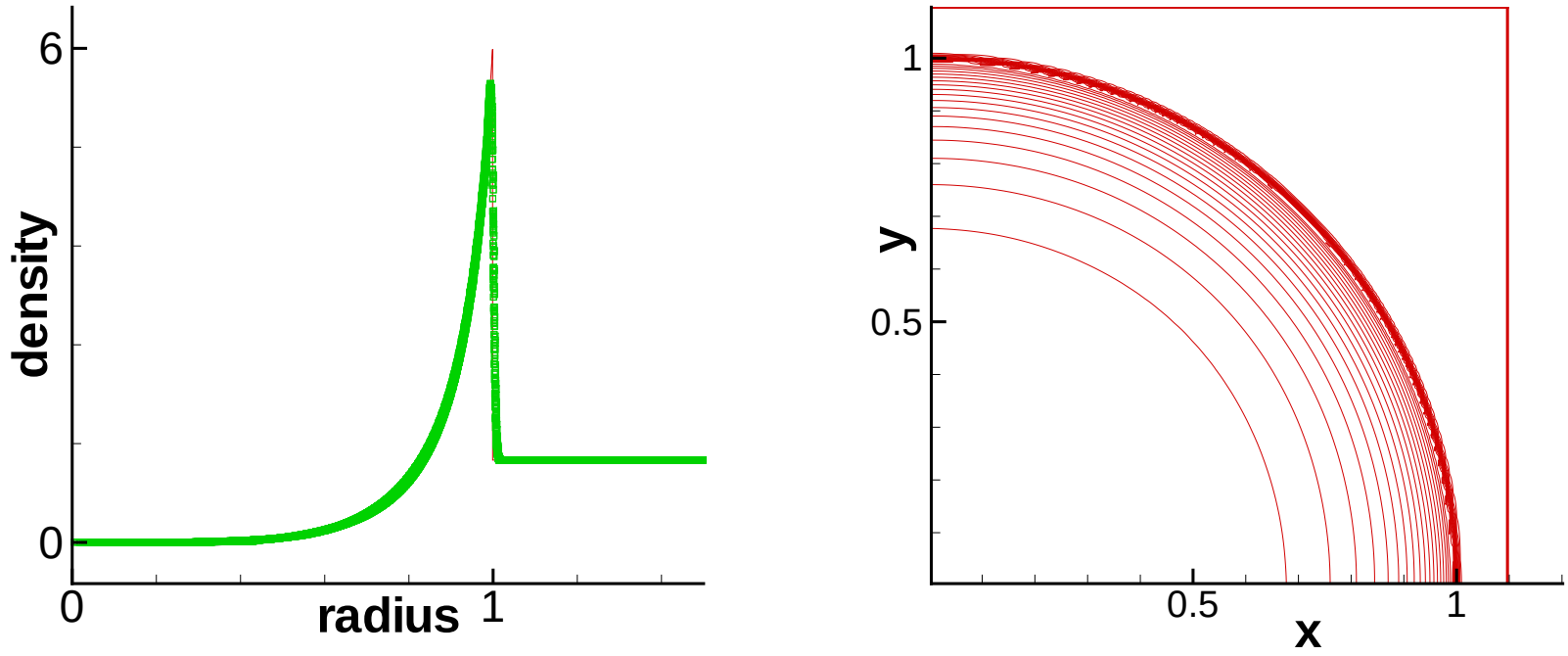

Figure 5: 2D Sedov blast, plot of density. $T = 1.$ $N = 160.$ $\Delta x = \Delta y = \frac{1.1}{N}$. TVB limiter parameters $(M_1, M_2, M_3, M_4) = (8000, 16000, 16000, 8000)$.

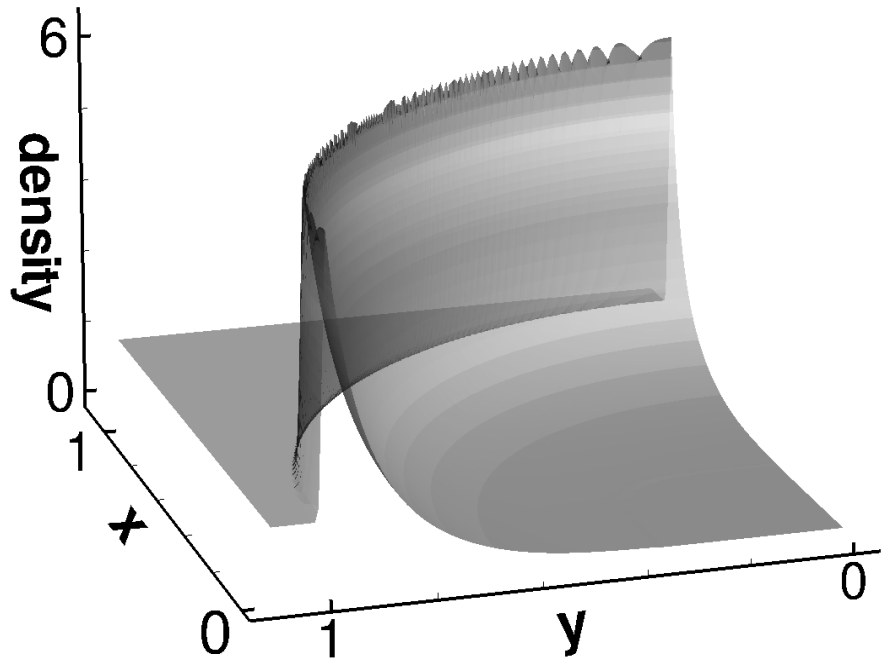

Figure 6: 2D Sedov blast, plot of density. $T = 1$. $N = 160$. $\Delta x = \Delta y = \frac{1.1}{N}$. TVB limiter parameters $(M_1, M_2, M_3, M_4) = (8000, 16000, 16000, 8000)$.

Example 5. We consider two Riemann problems. The first one is a double rarefaction. We did two tests, one is a one-dimensional double rarefaction, for which the initial condition is $\rho_L = \rho_R = 7, u_L = -1, u_R = 1,$ $p_L = p_R = 0.2$ and $\gamma = 1.4$. The other one is a two-dimensional double rarefaction with the initial condition $\rho_L = \rho_R = 7, u_L = -1, u_R = 1,$ $v_L = v_R = 0, p_L = p_R = 0.2$. The exact solution contains vacuum.

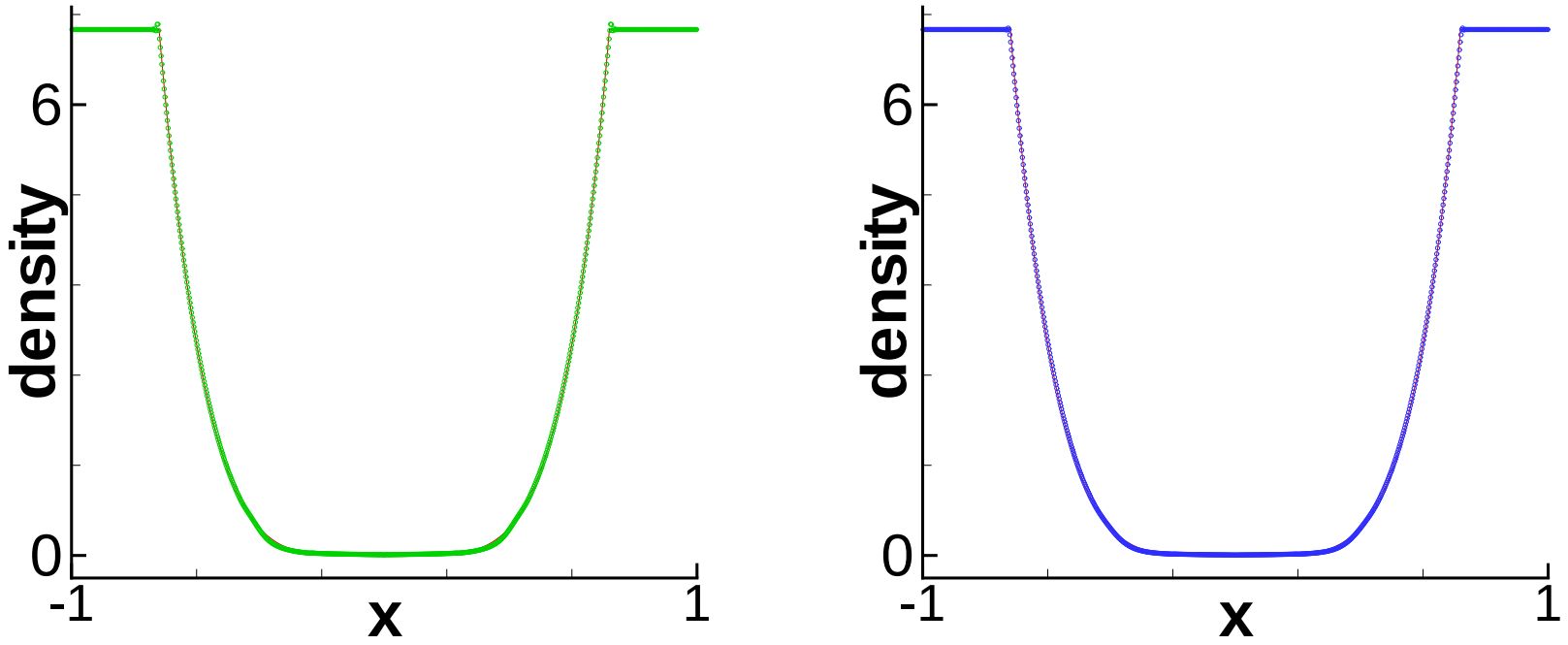

Figure 7: Double rarefaction problem. T=0.6. Left: 1D problem. Right: Cut at $y = 0$ for the 2D problem. Every fourth cell is plotted. The solid line is the exact solution. Symbols are numerical solutions. $\Delta x = \frac{2}{N}$, $N = 800$ with the positivity limiter. Density.

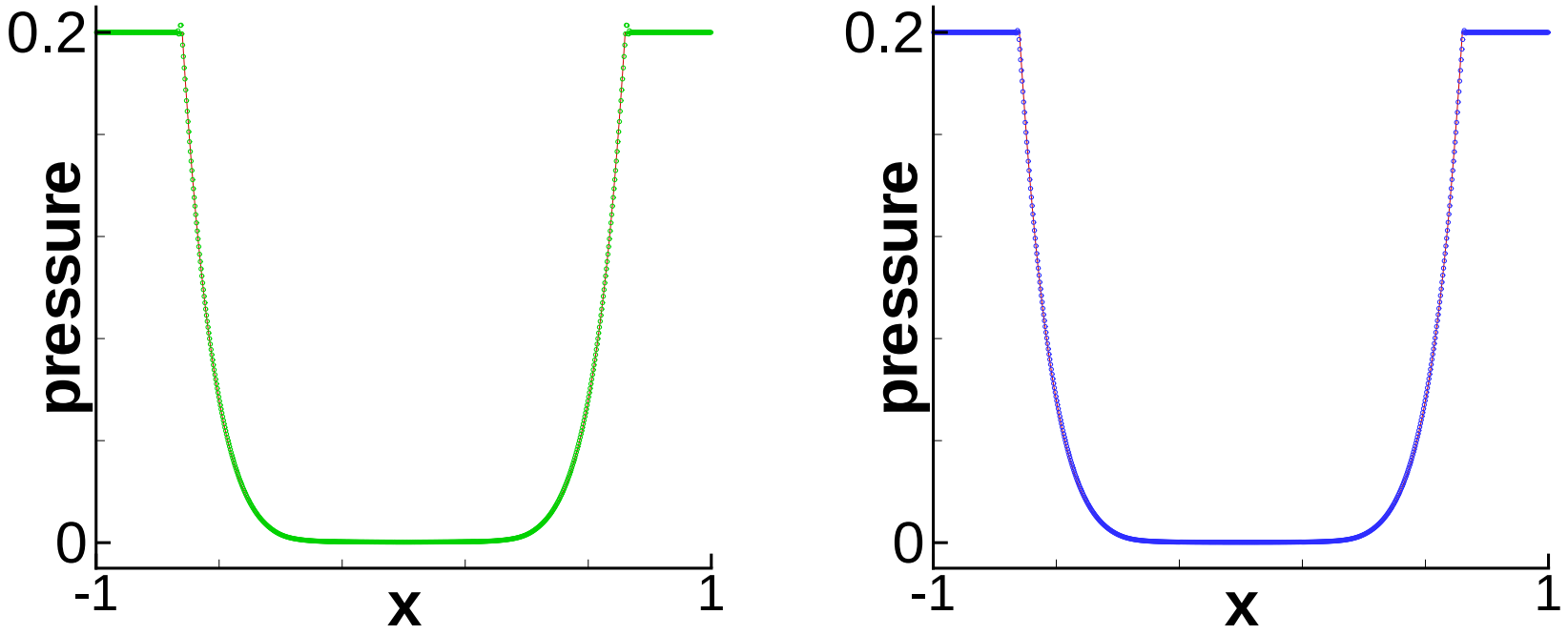

Figure 8: Double rarefaction problem. T=0.6. Left: 1D problem. Right: Cut at $y = 0$ for the 2D problem. Every fourth cell is plotted. The solid line is the exact solution. Symbols are numerical solutions. $\Delta x = \frac{2}{N}$, $N = 800$ with the positivity limiter. Pressure.

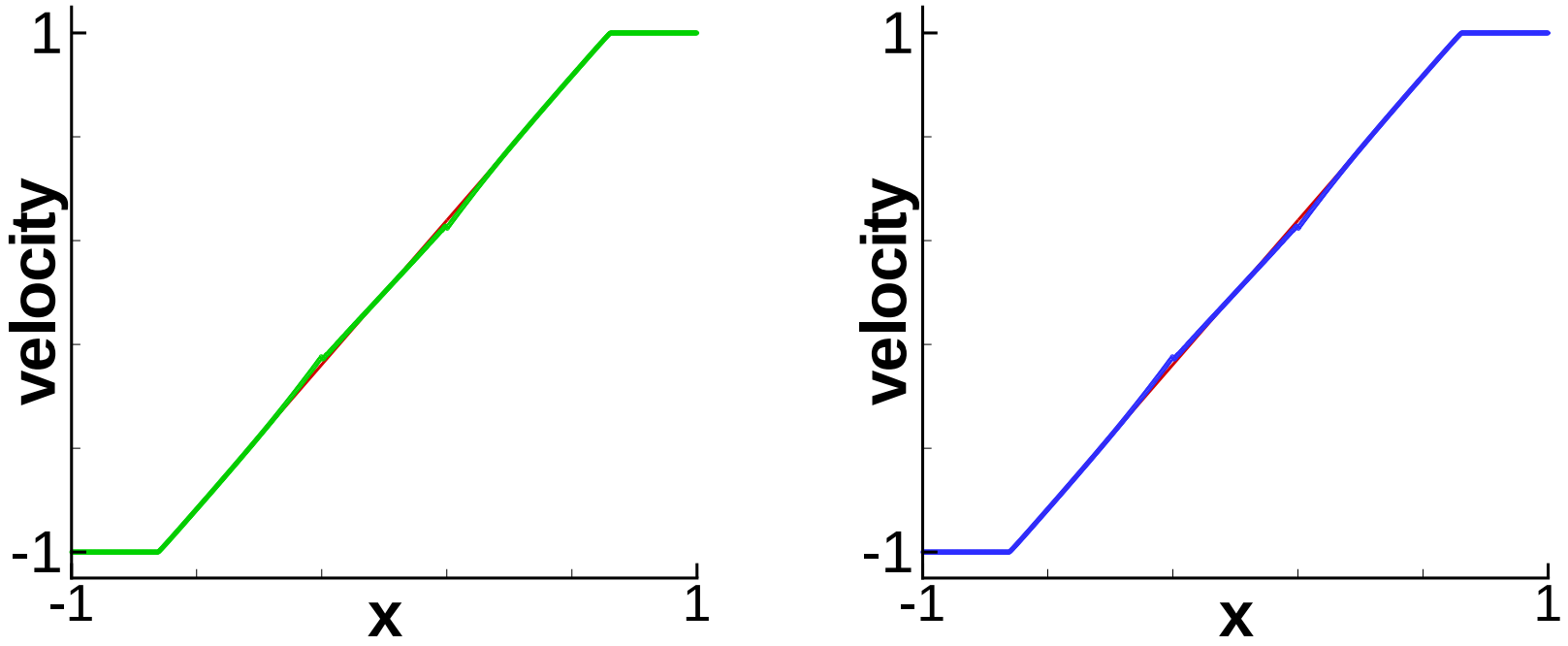

Figure 9: Double rarefaction problem. T=0.6. Left: 1D problem. Right: Cut at $y = 0$ for the 2D problem. Every fourth cell is plotted. The solid line is the exact solution. Symbols are numerical solutions. $\Delta x = \frac{2}{N}$, $N = 800$ with the positivity limiter. Velocity.

The second one is a 1D Leblanc shock tube problem. The initial condition is $\rho_L = 2$, $\rho_R = 0.001$, $u_L = u_R = 0$, $p_L = 10^9$, $p_R = 1$, and $\gamma = 1.4$. See the next figure for the results of 800 cells and 6400 cells.

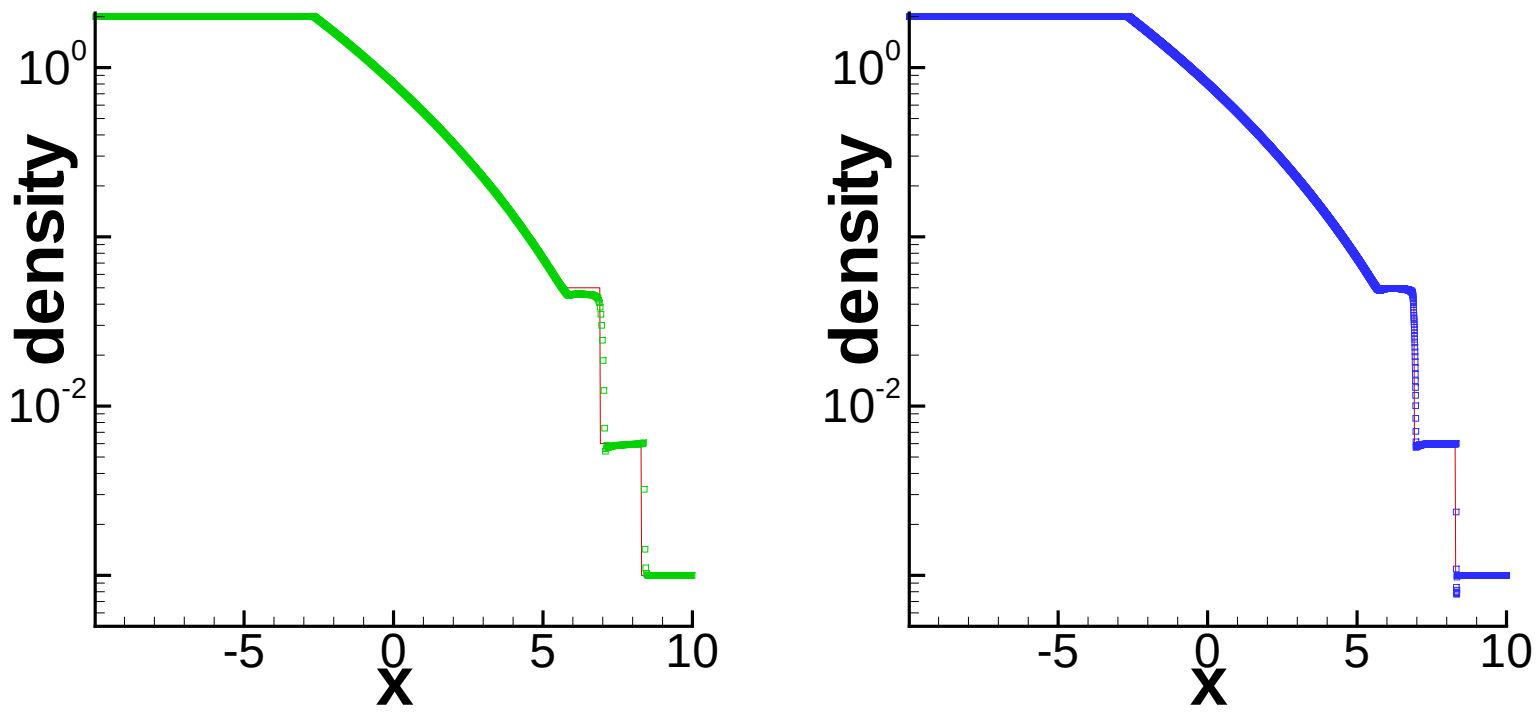

Figure 10: Leblanc problem. $T = 0.0001$. Left: $N = 800$. Right: $N = 6400$. The solid line is the exact solution. Symbols are numerical solutions. $\Delta x = \frac{20}{N}$ with the positivity limiter. $\log$-scale of density.

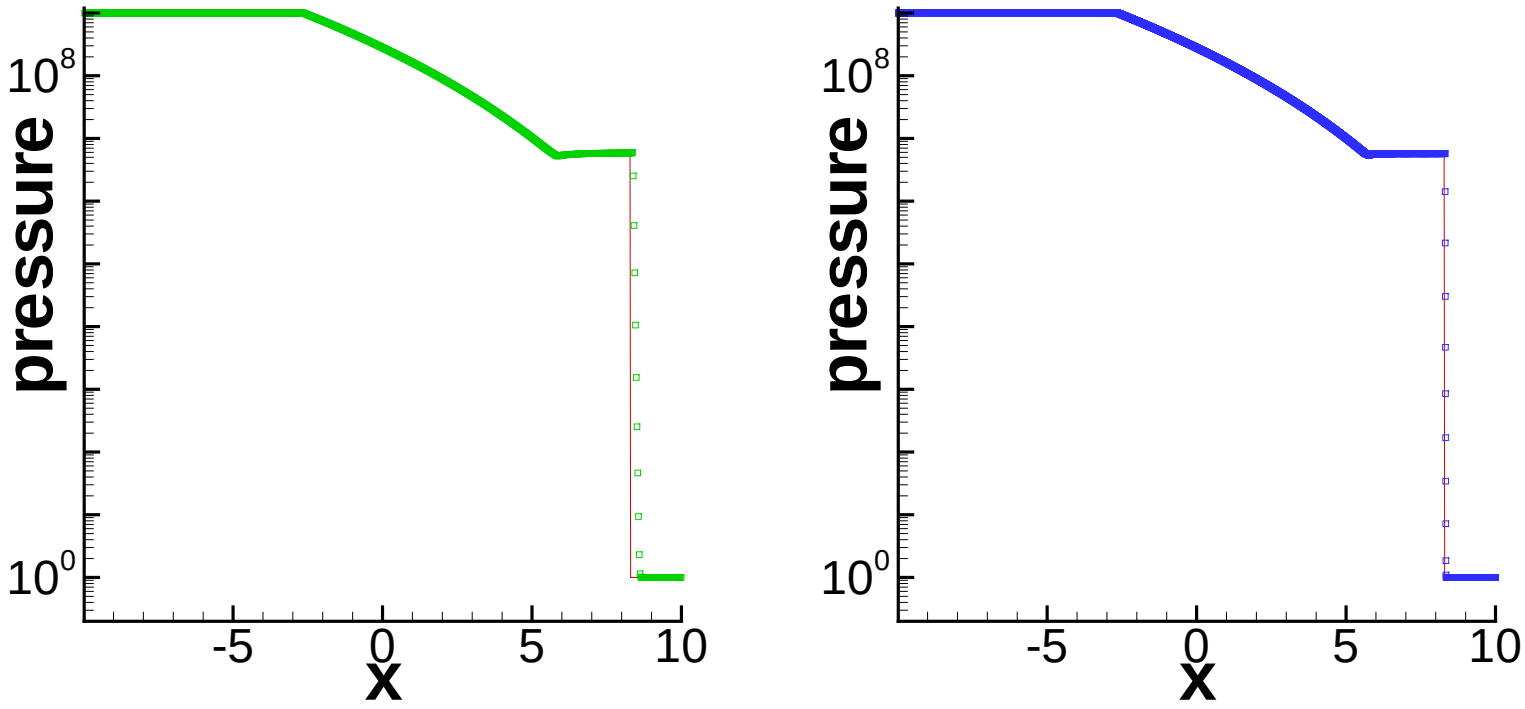

Figure 11: Leblanc problem. $T = 0.0001$. Left: $N = 800$. Right: $N = 6400$. The solid line is the exact solution. Symbols are numerical solutions. $\Delta x = \frac{20}{N}$ with the positivity limiter. $\log$-scale of pressure.

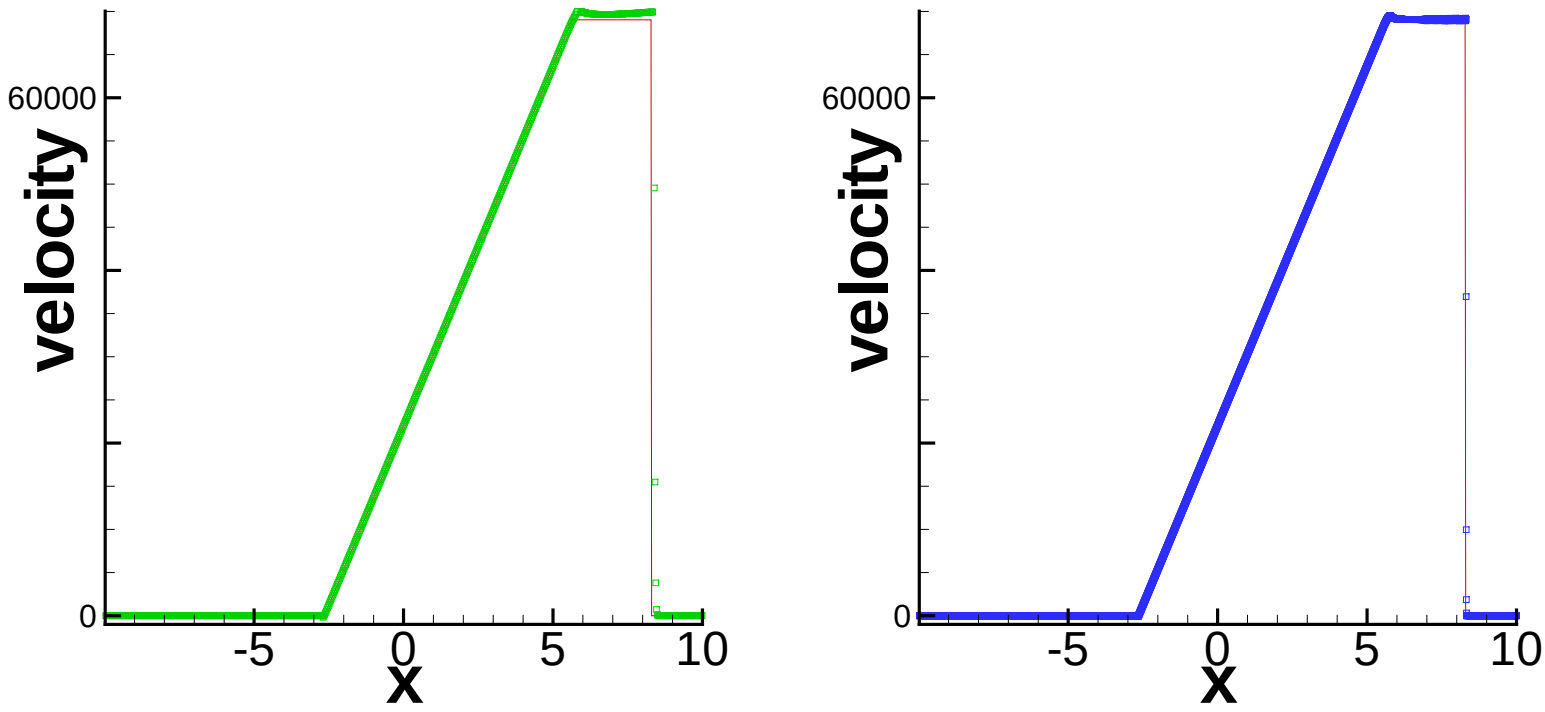

Figure 12: Leblanc problem. $T = 0.0001$. Left: $N = 800$. Right: $N = 6400$. The solid line is the exact solution. Symbols are numerical solutions. $\Delta x = \frac{20}{N}$ with the positivity limiter. Velocity.

Example 6. To simulate the gas flows and shock wave patterns which are revealed by the Hubble Space Telescope images, one can implement theoretical models in a gas dynamics simulator. The two-dimensional model without radiative cooling is governed by the compressible Euler equations. The velocity of the gas flow is extremely high, and the Mach number could be hundreds or thousands. A big challenge for computation is, even for a state-of-the-art high order scheme, negative pressure could appear since the internal energy is very small compared to the huge kinetic energy (Ha, Gardner, Gelb and Shu, JSC 2005).

First, we compute a Mach 80 (i.e. the Mach number of the jet inflow is 80 with respect to the soundspeed in the jet gas) problem without the radiative cooling.

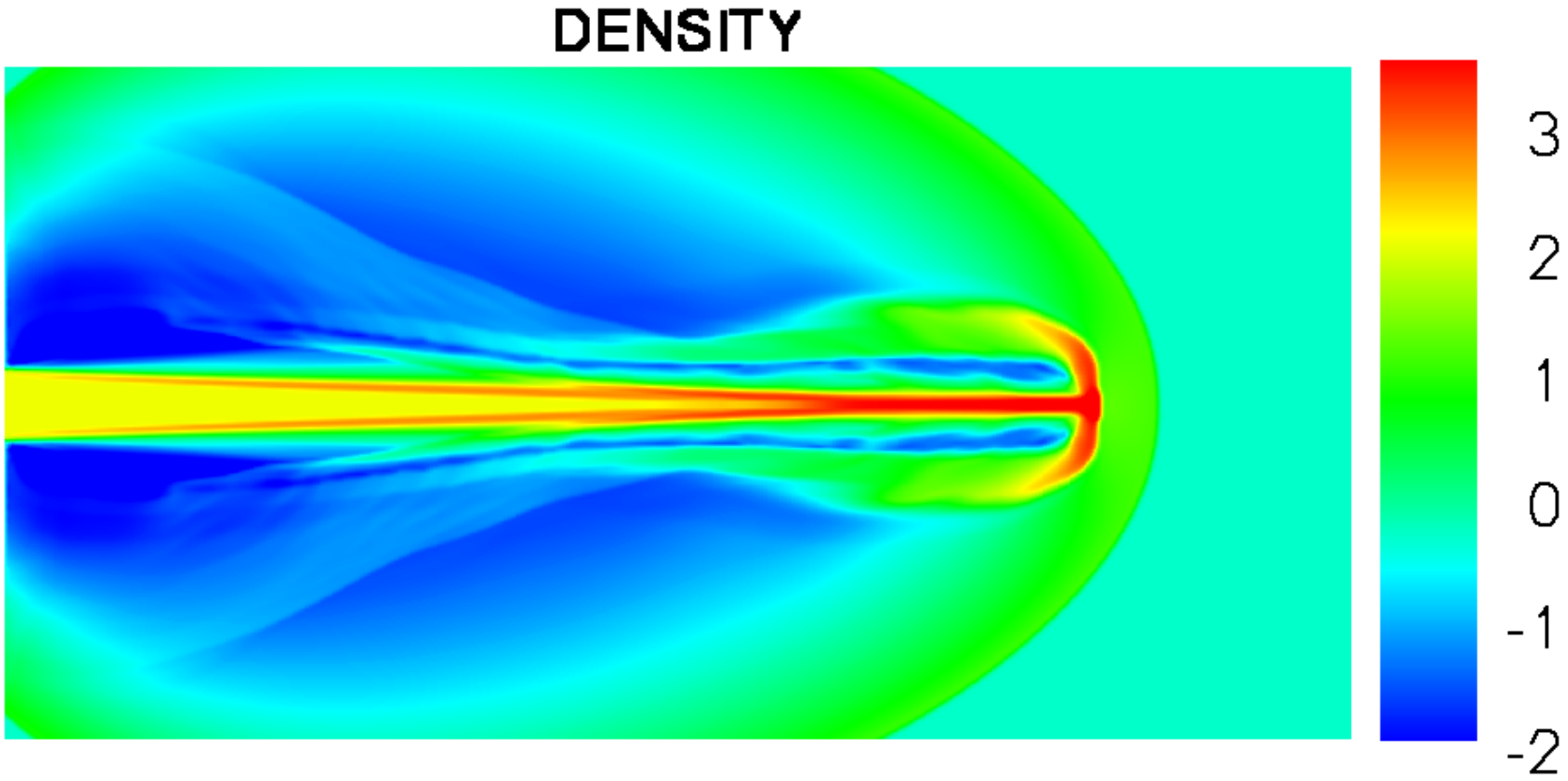

Figure 13: Simulation of Mach 80 jet without radiative cooling. Scales are logarithmic. Density.

Second, to demonstrate the robustness of our method, we compute a Mach 2000 problem. The domain is $[0, 1] \times [0, 0.5]$. The width of the jet is 0.1. The terminal time is 0.001. The speed of the jet is 800, which is around Mach 2100 with respect to the soundspeed in the jet gas. The computation is performed on a 640×320 mesh. TVB limiter parameters are $M_1 = M_2 = M_3 = M_4 = 10000000$.

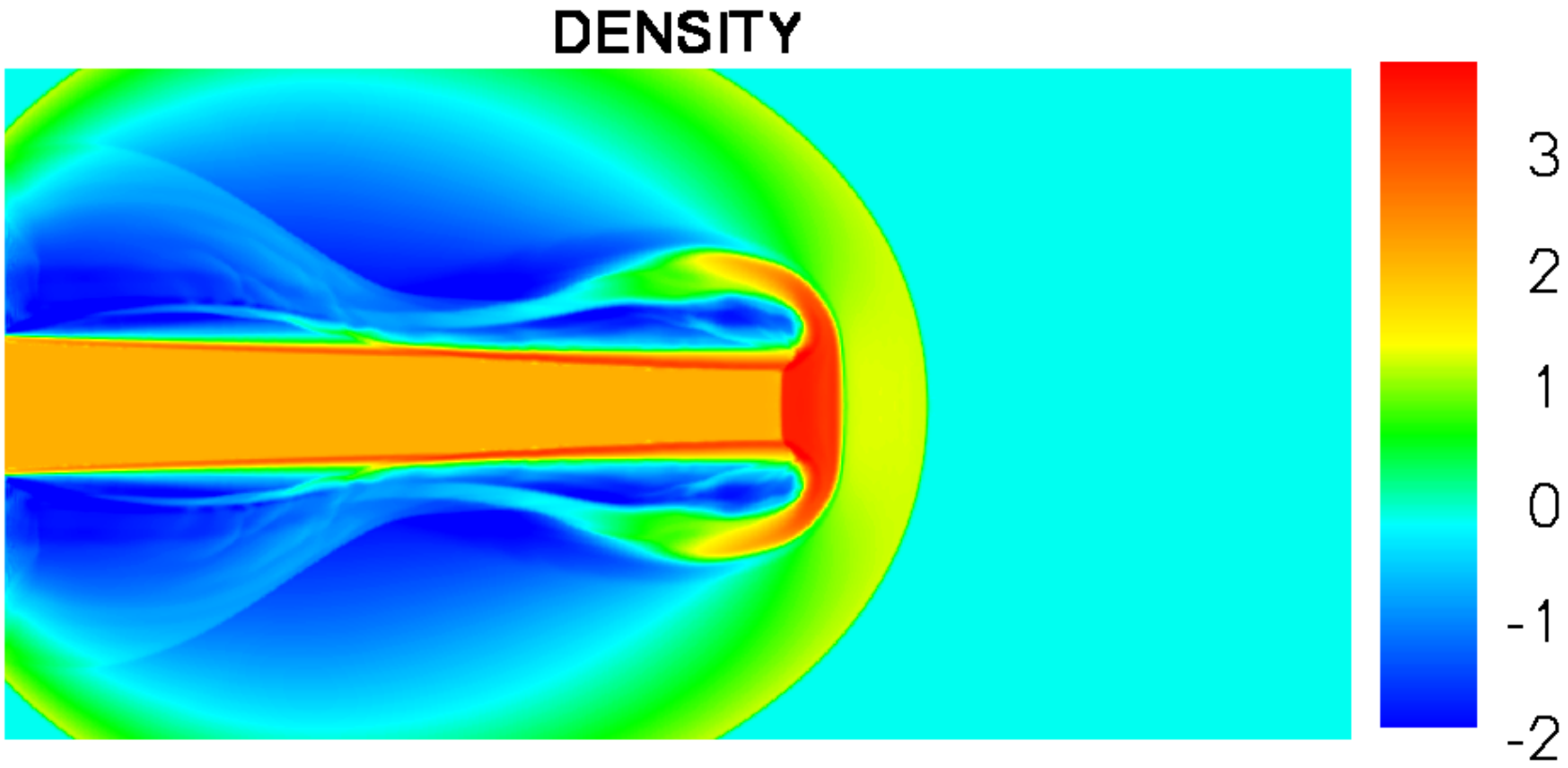

Figure 14: Simulation of Mach 2000 jet without radiative cooling. Scales are logarithmic. Density.

Lastly, we compute a Mach 80 (i.e. the Mach number of the jet inflow is 80 with respect to the soundspeed in the jet gas) problem with the radiative cooling to test the positivity-preserving property with the radiative cooling source term.

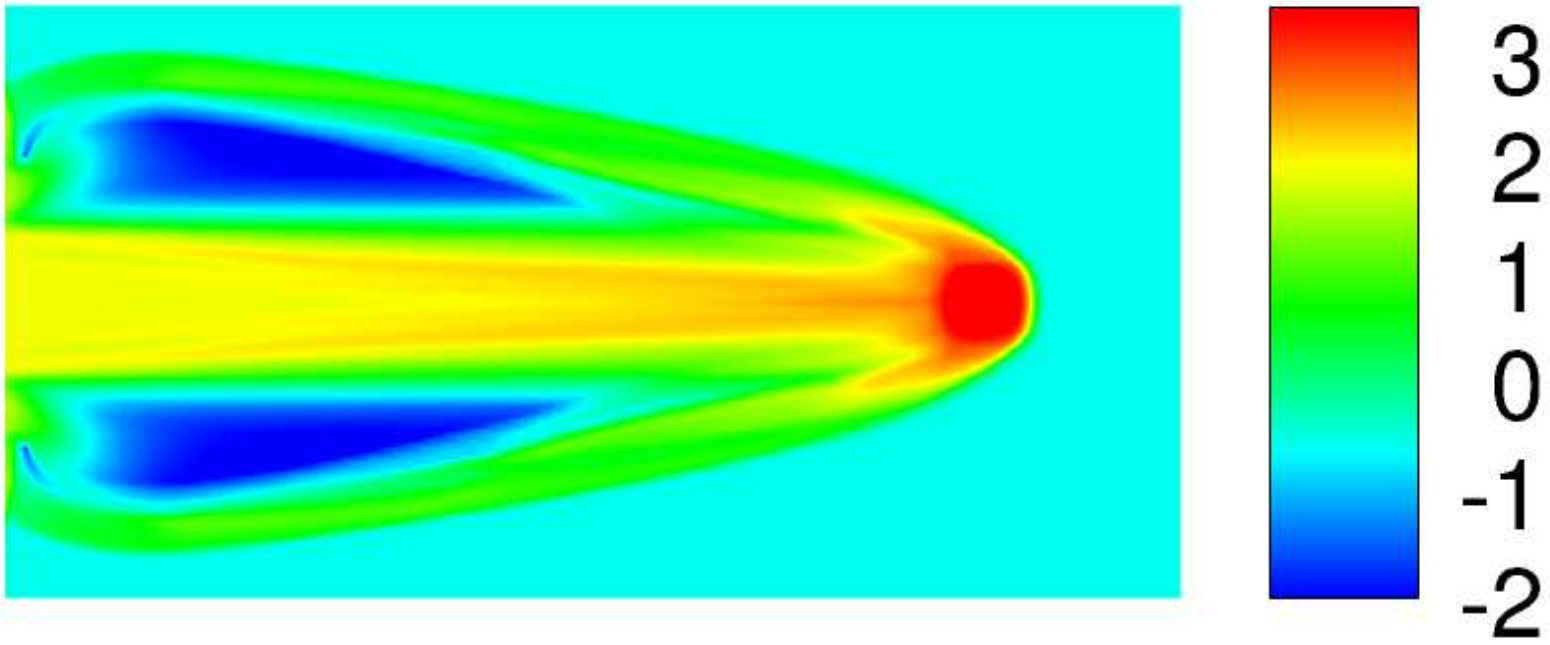

Figure 15: Simulation of Mach 80 jet with radiative cooling. The third order positivity-preserving RKDG scheme with the TVB limiter. Scales are logarithmic. Density.

Example 7. Shock diffraction problem. Shock passing a backward facing corner of 135°. It is easy to get negative density and/or pressure below the corner. This problem also involves mixed triangular / rectangular meshes for the DG method. The initial conditions are, if $x < 1.5$ and $y \geq 2$, $(\rho, u, v, E, Y) = (11, 6.18, 0, 970, 1)$; otherwise, $(\rho, u, v, E, Y) = (1, 0, 0, 55, 1)$. The boundary conditions are reflective. The terminal time is $t = 0.68$.

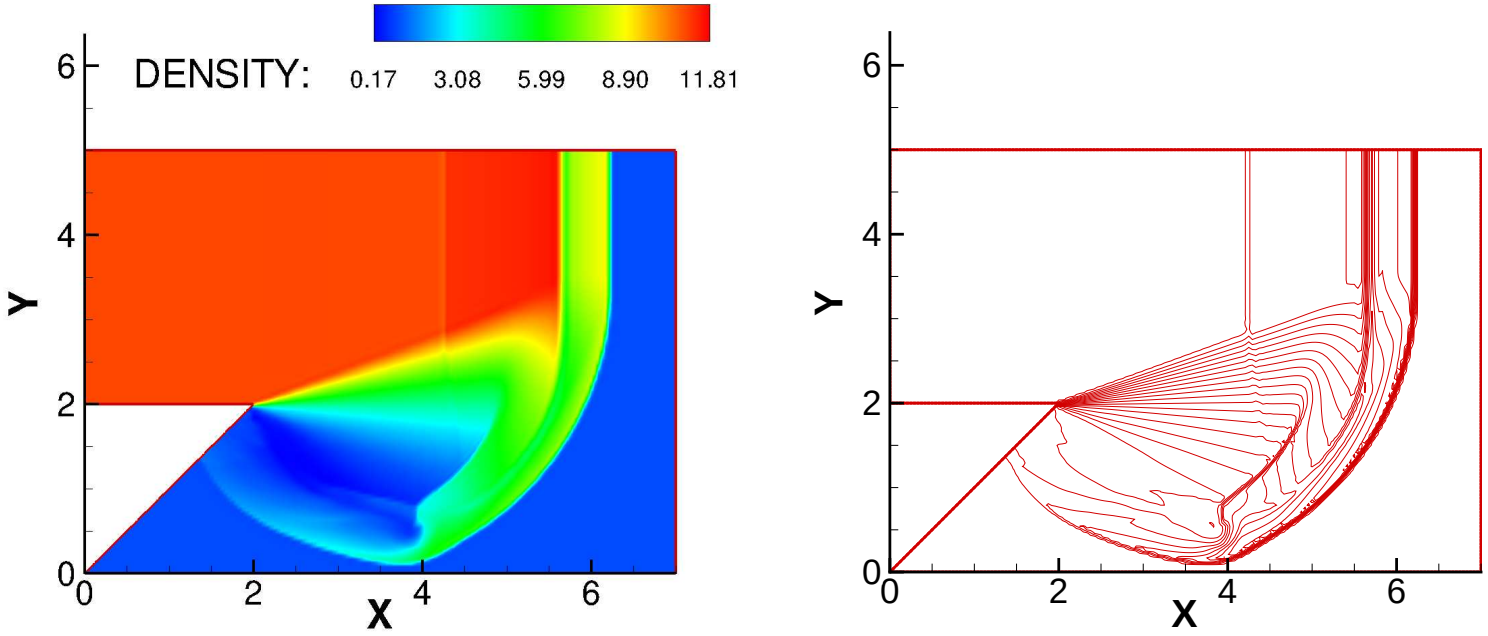

Figure 16: Density. Detonation diffraction at a 135° corner.

Conclusions and future work

- We have obtained uniformly high order bound-preserving schemes for multi-dimensional nonlinear conservation laws and convection-diffusion equations.
- In the future we will design higher order bound-preserving DG schemes for convection-diffusion equations on general triangulations, and for other types of PDEs.

The End

THANK YOU!